Correlations of Periodic, Area-Preserving Maps

James D. Meiss and John R. Cary
Institute for Fusion Studies,
University of Texas
Austin, Texas 78712

and

Celso Grebogi
Laboratory for Plasma and Fusion Energy Studies,
University of Maryland
College Park, Maryland 20742

and

John D. Crawford, Allan N. Kaufman, and Henry D.I. Abarbanel
Lawrence Berkeley Laboratory
University of California
Berkeley, California 94720

ABSTRACT

A simple analytical decay law for correlation functions of periodic, area-preserving maps is obtained. This law is compared with numerical experiments on the standard map. The agreement between experiment and theory is good when islands are absent, but poor when islands are present. When islands are present, the correlations have a long, slowly decaying tail.

I. Introduction

A primary goal of the theory of nonlinear dynamics is to understand the long time behavior of chaotic (nonintegrable) deterministic systems. As it is unlikely that one will be able to obtain a useful analytical representation of the individual trajectories of a nonintegrable system, and even numerical integration fails due to the stochastic instability, one can at best hope to provide a statistical description of families of orbits. Thus, there is great interest in the calculation of statistical quantities such as diffusion of orbits through phase space and decay of correlations.

The present work is concerned with the behavior of correlation functions and diffusion coefficients in two dimensional, periodic, area-preserving maps. Two-dimensional, area-preserving maps are obtained as approximate descriptions of many physical systems (such as particle accelerators, particles in magnetic mirrors and tokamaks) and quite generally as an exact reduction by surface of section of any two degree of freedom Hamiltonian. Furthermore, mappings are computationally the simplest of dynamical systems, and provide a testing ground for any theory.

In this paper we apply a formalism which was developed following the work of Rechester, Rosenbluth and White[6,7] to describe the statistical properties of maps. A statistical description is most readily accomplished in terms of probability functions; we calculate $k^{\underline{th}}$ joint probability $P_k(y_0,y_1,\ldots y_k)$ for a particle being at the points y_0, $y_1,\ldots y_k$ at the discrete times $t = 0,1,\ldots k$. To eliminate single orbit information, the probability is calculated as an average over initial conditions in some region, R, of phase space. Ideally the stochastic portion of phase space would be used as R; however, in practice this region is difficult to delineate. Therefore we typically let R be the

entire phase space, and so P_k includes information about both the regular and irregular orbits.

Application of our formalism is limited to periodic mappings, that is when the phase space is a torus. We consider maps of the form

$$p_{n+1} = p_n + \varepsilon f(x_n)$$

$$x_{n+1} = x_n + p_{n+1}$$

where $f(x+2\pi)=f(x)$. An example is the standard map[3], $f(x)=\sin x$. The primary quantity used is the Fourier transform of P_k (in each of the variables y_j) which is called the characteristic function, $\chi_k(\ell_0,\ell_1,\ldots\ell_k)$, in probability theory. Noting that the Fourier variables are discrete we obtain a recursion relation for χ_k which can be iterated yielding explicit formulae.[2]

Fourier space is useful for characterizing highly stochastic maps, since we expect the probability distribution to be nearly uniform in phase space. In this paper we exploit this by introducing an approximation for χ_k similar to the cumulant discard technique of turbulence theory. The recursion relation for χ_k shows that it is made up of products over lower order characteristic functions. Retaining only the second order characteristic functions yields a formula for χ_k (Eq. 7) like that for a high order moment when the cumulants have been neglected (e.g. as though the probability is gaussian). We call the terms retained principal terms, since they give the principal contribution to correlations in the stochastic limit.

Given the characteristic functions, or equivalently P_k, one can calculate any statistical quantity. As an example we calculate the force correlation functions and the momentum diffusion coefficient for the standard map.

To test our theory we have performed numerical experiments on the connected ergodic region of the standard map. (By the connected ergodic region we mean the ergodic region spanning several periods of the momentum-like variable.) The agreement between our simple analytical formulas and the numerical results is very good except at values of the nonlinearity parameter for which large islands are present or for which zero correlation time is predicted. When islands are present, the predicted exponential decay law fails at moderate time differences, and the correlation function develops long, significant tails. This is true even though the orbits never enter the island region. Enhancement of the diffusion constant is simultaneously observed.

This work should perhaps be compared with that of Karney et al.[4], who studied the standard map in the presence of extrinsic noise. They observed significant enhancement of the diffusion constant when islands were present. They attributed this enhancement to the noise-induced diffusion of orbits into islands. Obviously, this explanation does not apply to the present case, where KAM surfaces prevent orbits from entering islands.

II. Decay of Correlations: Principal Terms

The characteristic function formalism[1,2] gives exact expressions for correlation functions averaged over an invariant region of phase space. For ergodic regions, these expressions are equivalent to time-averaged correlations. Our formulas involve multiple sums over products of many functions and this obscures their behavior. In this section we present a heuristic technique for reducing these formulas to simpler expressions.

Our derivation uses the characteristic functions[1,2] defined by

$$\chi_k^R(\ell_k,\ell_{k-1},\ldots,\ell_1,\ell_0) \equiv \left\langle \exp\left[i \sum_{j=0}^{k} \ell_{k-j} x_j(x_0,p_0) \right] \right\rangle_R$$

where $x_j(x_0,p_0)$ is given as a function of the initial conditions through the map, and the average is over initial conditions (x_0,p_0) in the region R of phase space.

Using the mapping to determine $x_k = 2x_{k-1} - x_{k-2} + \varepsilon f(x_{k-1})$ in χ_k yields a recursion relation for characteristic functions. This relation can be iterated to obtain an explicit formula for χ_k. For the case of only two nonzero indicies this becomes [Eq. (14) of Ref. 2]:

$$\chi_k^R(\ell_k,0,0,\ldots,0,\ell_0) = \sum_{\substack{\ell_1,\ell_2,\ldots \\ \ell_{k-1}=-\infty}}^{\infty} \prod_{j=0}^{k-2} g_{\nu_j}(\varepsilon \ell_j) \chi_1^R(\ell_k - \ell_{k-2}, \ell_{k-1}), \qquad (1)$$

where $\ell_{-1} = 0$,

$$\nu_j = \ell_{j-1} - 2\ell_j + \ell_{j+1} , \qquad (2)$$

and g_ℓ is defined by

$$\exp[i\varepsilon f(x)] = \sum_{\ell=-\infty}^{\infty} g_\ell(\varepsilon)\, \exp(i\ell x).$$

We assume $f(x) = -f(-x)$, which is valid for the standard map[3], so that

$$g_{-\ell}(-\varepsilon) = g_\ell(\varepsilon) = g_\ell^*(\varepsilon). \tag{3}$$

The expression (1) is valid for an arbitrary invariant region, R, of phase space, but we specialize to the case $R = [-\pi,\pi] \times [-\pi,\pi]$, which is the entire (reduced) phase space. In this case

$$\chi_1^R(m,n) = \delta_{m,0}\, \delta_{n,0}. \tag{4}$$

Thus we are considering properties averaged over all orbits: only if the map is ergodic would this be equivalent to a single orbit time average. In principle one could let R be the connected stochastic region of the map (for ε large) and then only Eq. (4) would need to be altered. Recalling that the measure of regular motion for the standard map is estimated to be $O(1/\varepsilon^2)$, one notes that Eq. (4) will need a correction of this order if the irregular region is used.

We wish to obtain an approximate expression for Eq. (1) when $\varepsilon \gg 1$. We note that $g_0(0) = 1$, and that for smooth force functions f, one generally has

$$g_\nu(\varepsilon\ell) \ll 1 \tag{5}$$

when $(\nu,\ell) \neq (0,0)$. An example is the standard map, where $g_\nu(\varepsilon) = J_\nu(\varepsilon)$. One can show

$$\max_x [J_\nu(x)] \lesssim C\, \nu^{-1/3}$$

for $\nu \gg 1$, on the basis of Ref. 5. [See Eq. (A6) of the appendix.] Thus, of all the terms in Eq. (1), those with ν_j small are the largest. To capitalize on this we approximate Eq.(1) by keeping only terms with ν_j small. The most extreme truncation is to set the ν_j's to zero; however, Eq. (2) restricts the number of such terms. The principal terms are defined as those with the maximum number of factors, $g_\nu(\ell\varepsilon)$, equal to unity. This requires $\ell_j = \nu_j = 0$ for each such factor. The index ℓ_0 is fixed in Eq. (1), so we start by setting $\ell_1 = \nu_1 = 0$. These conditions imply $\ell_2 = -\ell_0$, thus fixing ℓ_2. We next set $\ell_3 = \nu_3 = 0$ and so on. Proceeding in this fashion, we set $\nu_j = \ell_j = 0$ for all odd j and obtain $(\ell_2, \nu_2) = (-\ell_0, 2\ell_0)$, $(\ell_4, \nu_4) = (\ell_0, -2\ell_0)$, $(\ell_6, \nu_6) = (-\ell_0, 2\ell_0)$, etc. . This choice of the indices ℓ_j is represented pictorially in Fig. 1 as a trajectory in (j,ℓ) space. These trajectories should not be confused with the Fourier-space paths of Refs.6 and 7.

The trajectory terminates at $j = k-2$ with $\ell_{k-2} = \ell_k$, according to Eqs. (1) and (4). To obtain a nontrivial result, we need $\ell_k \neq 0$. Therefore, we find that k must be even, and $\ell_k = (-1)^{(k-2)/2}\ell_0$. This principal term is actually a single term in the multiple sums of (1) which has k/2 factors of g's with nonzero indices:

$$\chi_k^P(\ell_k, 0, 0, \ldots, \ell_0) = [g_{-2\ell_0}(\ell_0\varepsilon)]^{k/2}\, \delta_{\ell_0, (-1)^{(k-2)/2}\ell_k}. \qquad (6)$$

This result is exact for k=0 and 2.

A similar analysis may be used to obtain χ_k with k odd, except that the (j,ℓ) trajectory must contain a single "defect", i.e. a single odd j for which either ℓ_j or ν_j is not zero. Figure 2 shows a trajectory with a defect at $j = j_D$, where j_D is odd and $\ell_{j_D} \neq 0$. It is clear from Fig. 2 that $\ell_{j_D-1} =$

$(-1)^{(j_D-1)/2}\ell_0$ and $\ell_{j_D} = (-1)^{(k-2-j_D)/2}\ell_k$. The presence of the defect relaxes the endpoint restriction $|\ell_k| = |\ell_0|$.

Keeping all such single-defect terms for the odd-k correlations of Eq. (1), we obtain

$$\chi_k^P = [g_{-2\ell_k}(\varepsilon\ell_k)]^{\frac{k-3}{2}} \sum_{m=0}^{\frac{k-3}{2}} \left(\frac{g_{-2\ell_0}(\varepsilon\ell_0)}{g_{-2\ell_k}(\varepsilon\ell_k)} \right)^m$$

$$\times \begin{cases} g_{\ell_k-2\ell_0}(\varepsilon\ell_0) g_{\ell_0-2\ell_k}(\varepsilon\ell_k) & \text{for } \frac{k+1}{2} \text{ even} \\ g_{\ell_k+2\ell_0}(-\varepsilon\ell_0) g_{\ell_0+2\ell_k}(-\varepsilon\ell_k) & \text{for } \frac{k+1}{2} \text{ odd} \end{cases} .$$

Specializing to the case $|\ell_k| = |\ell_0|$, which is all that is needed for the force-correlation function[2], we obtain

$$\chi_k^P(\pm\ell_0,0,0,\ldots,\ell_0) = \frac{k-1}{2}[g_{-2\ell_0}(\varepsilon\ell_0)]^{\frac{k-3}{2}} \begin{cases} [g_{-\ell_0}(\varepsilon\ell_0)]^2 & ,(7a) \\ [g_{-3\ell_0}(\varepsilon\ell_0)]^2 & ,(7b) \end{cases}$$

for (k+1)/2 even. The upper and lower expressions (valid for $\ell_k = \pm\ell_0$ respectively) are interchanged when (k+1)/2 is odd.

We now specialize to the standard map, for which the force correlation is given by (see Ref. 2)

$$C_k = \langle f(x_k)f(x_0)\rangle_R = \langle \sin(x_k)\sin(x_0)\rangle_R$$

$$= \frac{1}{2}[\chi_k(1,0,0,\ldots,0,-1) - \chi_k(1,0,0,\ldots,0,1)].$$

Using the results (6) and (7), we obtain the principal term contribution

$$C_k^P = \begin{cases} \frac{1}{2}\,[-J_2(\varepsilon)]^{k/2} & \text{for } k \text{ even} \\ -\frac{k-1}{k+1}\,\frac{4}{\varepsilon}\,\frac{d}{d\varepsilon}\,[-J_2(\varepsilon)]^{\frac{k+1}{2}} & \text{for } k \text{ odd.} \end{cases} \tag{8}$$

These expressions are exact for $k < 4$.

The odd-k correlations are normally much smaller than the even-k correlations when ε is large. From Eq. (8) we have

$$\left| \frac{C_{k+1}}{C_k} \right| = 4\,\frac{k}{\varepsilon}\,|J_2'(\varepsilon)| \lesssim 4k\left(\frac{2}{\pi\varepsilon^3}\right)^{1/2},$$

while

$$\left|\frac{C_{k+2}}{C_k}\right| = |J_2(\varepsilon)| \lesssim \left(\frac{2}{\pi\varepsilon}\right)^{1/2}.$$

for ε large and k even.

An estimate for the error in χ_k^P is obtained by considering the defect correction for k even. Suppose the trajectory of Fig. 1 has a defect as some odd j_D (even j_D defects give zero contribution). Since the defect can occur at any odd j_D the correction is k-2/2 times the value at one, and furthermore the index ℓ_{j_D} must now be summed over. This correction gives the error estimate

$$\frac{\Delta\chi_k}{\chi_k} \simeq \frac{k-2}{2}\left[\frac{\chi_4(1,0,0,0,-1)}{\chi_4^P(1,0,0,0,-1)} - 1\right] \tag{9}$$

involving the exact value of the fourth characteristic function. Since defects occur at any position on the trajectory, the error grows with k, and the principal term expression is valid only for $k < k_{max}(\varepsilon)$. In Fig. 3 we plot computations of $\chi_4 - \chi_4^P$ and k_{max} (given by setting Eq. (9) to one) as a function of ε. The graph of χ_4 shows three broad peaks near $\varepsilon = 2\pi n$ which correspond to regions where first order islands are present.[3] In addition many of the narrower peaks occur in conjunction with second order islands.[4] Thus we expect large error in χ_k^P whenever islands exist. The error is also large near $\chi_4^P = 0$, and this is reflected in $k_{max} \to 2$ at the zeros of $J_2(\varepsilon)$ in Fig. 3b. This graph predicts $k_{max} \sim 7$, with of course many oscillations, except near $J_2 = 0$.

The principle value for the diffusion constant is obtained by using Eq. (8) in the representation of the diffusion constant as a sum of force correlations [Ref.2, Eq. (16)]. The result is

$$D^P = \frac{\varepsilon^2}{4} \quad \frac{1-2J_1^2(\varepsilon)-J_2^2(\varepsilon)+2J_3^2(\varepsilon)}{[1+J_2(\varepsilon)]^2} \quad . \tag{10}$$

While there are corrections to Eq. (10) containing products of three Bessel functions, this result is an improvement over previous work[6,7] in that certain terms have been summed to all orders in $\varepsilon^{-1/2}$ giving the denominator. Our argument to obtain Eq. (10) is similar in spirit to a renormalization since we keep one infinite set of terms, discarding the rest.

Finally, we note that the principal-terms argument can be used to obtain values for other correlations as well. As an example, consider the sin(p) correlations,

$$C_j^{\sin p} \equiv \langle \sin(p_i)\, \sin(p_{i+j}) \rangle$$

$$= \frac{1}{2} [\chi_{j+1}(-1,1,0,0,\ldots,0,1,-1) - \chi_{j+1}(-1,1,0,0,\ldots,0,-1,1)]. \quad (11)$$

Now the generalization of Eq. (1) to the case of two nonzero ending indices must be used:

$$\chi_k^R(\ell_k,-\ell_{k+1},0,0,\ldots,0,-\ell_{-1},\ell_0) =$$

$$\sum_{\ell_1,\ell_2,\ldots,\ell_{k-1}} \prod_{j=0}^{k-2} g_{\nu_j}(\varepsilon\ell_j)\chi_1^R(\ell_k-\ell_{k-2},\ell_{k-1}-\ell_{k+1}) \quad (12)$$

The principal terms argument now gives

$$C_j^{\sin p} = -\frac{1}{2} [J_1(\varepsilon)]^2 [-J_2(\varepsilon)]^{\frac{j-3}{2}} \quad (13)$$

for j odd and greater than two. The even-j correlations are much smaller when $\varepsilon \gg 1$.

III. Experiments

A. Measuring procedure

To compare with the theory, a series of measurements of the diffusion constant and the correlation functions of the connected ergodic region were performed. These numerical measurements were performed on the Digital VAX11/780 computer with double precision arithmetic and checked with calculations on the CDC 7600 computer with single precision arithmetic.

Correlation functions were measured by averaging over a single orbit of length N in the connected ergodic region.

$$C_j \equiv \frac{1}{N} \sum_{i=1}^{N} \sin x_i \sin x_{i+j} \tag{14}$$

The uncertainty of the correlation function was taken to be the standard deviation of the mean,

$$\sigma_j \equiv \left[\frac{1}{N^2} \sum_{i=1}^{N} (\sin x_i \sin x_{i+j})^2 - C_j^2/N \right]^{1/2}. \tag{15}$$

The correlation function is usually defined with the product of the means subtracted out, i.e.

$$C_j' \equiv C_j - \left(\frac{1}{N} \sum_{i=1}^{N} \sin x_i \right)^2 ;$$

however, the last term in this equation was found to be small for all cases.

The expression (15) for the error relies on the separate terms in the sum of Eq. (14) being independent measurements of the correlation function. This assumption is actually false if the correlation time is significant, since neighboring terms in the sum are then not independent. For most of the following measurements, the correlation time is short, so that Eq. (15) is accurate. However, for the cases of long correlation times, Eq. (15) should be regarded as a rough estimate.

The diffusion constant was measured for a single orbit of length N in the connected ergodic region by breaking the orbit into n suborbits of length T (N=nT). The initial and final momenta of a suborbit provide a single measurement of the diffusion constant according to

$$D_i = \frac{1}{2T} (p_{iT} - p_{(i-1)T})^2 .$$

Of course, the uncertainty of this single measurement is unknown. To find the best value of the diffusion constant, we average the value from each of the suborbits.

$$D \equiv \frac{1}{n} \sum_{i=1}^{n} D_i \qquad (16)$$

The uncertainty in the diffusion constant was taken to be given by

the standard deviation of the mean,

$$\sigma_D \equiv \frac{1}{n}\left[\sum_{i=1}^{n} D_i^2 - \frac{1}{n}\left(\sum_{i=1}^{n} D_i\right)^2\right]^{1/2} . \qquad (17)$$

In the case the error expression is accurate provided T is chosen large enough to make the separate measurements of the diffusion constant independent.

It might be argued that the use of these statistical formulas is incorrect for a deterministic system. However, this point was checked by comparing runs of various lengths with various initial conditions. It was found that the formula (15) for the uncertainty was consistent with the measurements.

Although the final measurement was made on a single, very long orbit, various checks were performed to insure that this orbit was not peculiar. Shorter runs with different orbit and suborbit lengths and different initial conditions were made. These were compared to make certain the measurements were consistent. Furthermore, surface of section plots were made to verify the ergodicity of the orbit.

B. Results

Figures 4-6 compare the numerically obtained force correlations with the principal-terms result (8) for the standard map at various values of ε. All of these measurements were made using orbits of length $N = 3.5 \times 10^7$. The uncertainty of the numerical measurement as given by Eq. (15) is indicated by the vertical bar. The uncertainty is found to scale with $N^{-1/2}$.

Figure 4 shows the absolute value of the numerically obtained force-correlation function for the standard map at $\varepsilon = 10.5$. The solid line in the graphs is the principle-terms value $|C_k^P| = \frac{1}{2} |J_2(\varepsilon)|^{k/2}$ which is valid for the even-k terms. At this value for ε, the force-correlation decays rapidly and is in good agreement with the principle-terms result.

Figure 5 shows the numerically obtained force-correlation function for the standard map at $\varepsilon = 11.5$. Again the principal-terms value for the even correlations is drawn. At this value of ε, the force correlation decays rapidly, but it is not in good agreement with the principle terms result. The reason for this disagreement is that J_2 is near a zero at $\varepsilon = 11.5$. Hence, the argument that terms with $J_2(\varepsilon)$ dominate is incorrect.

Figure 6 shows the numerically obtained force correlation function for the standard map at $\varepsilon = 12.8$. Now the correlation function decays very slowly. It appears to have a long, low-level tail. Obviously, the agreement with the principal-terms result is poor. At this value of ε, the standard map has accelerator modes, islands in which the particles experience perpetual acceleration.[3] Even though the measured orbit was never in the accelerator mode, its correlation function was affected.

This pattern was observed in many other measurements. The principal terms give good values for the force correlations if ε is not at or near a value for which there are islands, or for which $J_2(\varepsilon)$ is nearly zero. Furthermore, the force correlations tend to decay quickly, even for modest values of ε, unless there are islands present. This pattern was also observed for other correlations such as the sin(p) correlations of Eq. (13).

To better understand these force correlations we also measured the diffusion constant, which is a sum of all of the correlations [see Ref. 2, Eq. (16)]. The numerical results for the diffusion constant normalized to the quasilinear value, $D_{QL} = \frac{1}{4}\varepsilon^2$, are shown in Fig. 7. These measurements were made by averaging 3500 suborbits of 10^4 time steps, i.e. n = 3500 and T = 10^4. The circled experimental points correspond to values of ε for which there exist first or second order islands (see Ref. 4, Table I). The solid curve is the theoretical result, Eq. (10). The dashed curve is the low order result $D = 1-2J_2(\varepsilon)$.

It is clear from Fig. 7 that the agreement between theory and numerical experiment is excellent as long as islands are absent. Furthermore, the discrepancy due to islands or other effects diminishes with ε. Of course, the theory must break down when islands are present, in which case the wrong region R (see Ref. 1) has been used for the average. Moreover, the series must diverge when accelerator regions are present, because the series averages in the infinite diffusion of the accelerator regions. Hence, the series for the diffusion constant should be viewed as an asymptotic series, for which it is best to keep a limited number of terms.

We mention in passing that the presence of islands appears to cause quite a few anomalies in the numerical measurement of the diffusion constant. As shown in Fig. 7, the diffusion constant can be an order of magnitude larger than the quasilinear value when islands are present. Secondly, the error, as given by Eq.

(17), is very large. Finally, suborbits of 10^4 time steps do not appear to be long enough to determine D when islands are present. This was inferred from the fact that the measurement of D depends on T even for $T \cong 10^4$.

IV. Conclusions

The characteristic function method can be used to obtain approximate expressions for the moderate time correlations provided the accelerator modes are absent or insignificant. When accelerator modes are absent, the correlation functions decay rapidly and the diffusion constant is given by Eq. (10). The presence of accelerator modes coincides with long tails in the correlation functions of the connected ergodic region and much larger values of the diffusion constant.

V. Acknowledgements

The authors would like to thank Dr. C.F.F. Karney for several useful discussions. This work was supported by the U.S. Department of Energy under contracts DE FG05-80ET-53088, W-7405-ENG-48, and DE AC05-79ET-53044 (Office of Basic Energy Sciences).

Appendix

A uniform asymptotic expansion of the Bessel function for real positive z is[5]

$$J_\nu(\nu z) \sim \nu^{-1/3}\left(\frac{4\zeta}{1-z^2}\right)^{\frac{1}{4}} \mathrm{Ai}\left(\nu^{2/3}\zeta\right) + \mathcal{O}\left(\nu^{-5/3}\right), \tag{A1}$$

where ζ is the real root of

$$\zeta = \left\{ \frac{3}{2}\left[\ell n\left(1+(1-z^2)^{1/2}\right) - \ell n\, z - (1-z^2)^{1/2}\right]\right\}^{2/3} \tag{A2}$$

for $z < 1$, and of

$$\zeta = -\left\{\frac{3}{2}\left[(z^2-1)^{1/2} - \arccos(z^{-1})\right]\right\}^{2/3} \tag{A3}$$

for $z>1$. This result allows us to derive a uniform bound for $J_\nu(z)$ for large order.

We first consider the region $z>\eta$, where $0<\eta<1$. We find

$$\underset{z>\eta}{\mathrm{Max}}\ |J_\nu(\nu z)| < \nu^{-1/3} \underset{z>\eta}{\mathrm{Max}}\ \left(\frac{4\zeta}{1-z^2}\right)^{\frac{1}{4}} \underset{z>0}{\mathrm{Max}}\ \mathrm{Ai}(\nu^{2/3}\zeta) + \mathcal{O}(\nu^{-5/3}).$$

Therefore,

$$\underset{z>\eta}{\mathrm{Max}}|J_\nu(\nu z)| < C_1(\eta)\nu^{-1/3} + \mathcal{O}(\nu^{-5/3}). \tag{A4}$$

where C_1 is independent of ν.

In the remaining region, $z<\eta$, we have

$$\underset{z<\eta}{\text{Max}}|J_\nu(\nu z)| < \nu^{-1/2}\left[4/(1-\eta^2)\right]^{1/4} \underset{z<\eta}{\text{Max}}\left[(\nu^{2/3}\zeta)^{1/4}\text{Ai}(\nu^{2/3}\zeta)\right] + \mathcal{O}(\nu^{-5/3})$$

$$< \nu^{-1/2}\left[4/(1-\eta^2)\right]^{1/4} \underset{y>0}{\text{Max}}\, y^{1/4}\text{Ai}(y) + \mathcal{O}(\nu^{-5/3})$$

Thus we deduce

$$\underset{z<\eta}{\text{Max}}\,|J_\nu(\nu z)| < C_2(\eta)\nu^{-1/2} + \mathcal{O}(\nu^{-5/3}), \tag{A5}$$

where $C_2(\eta)$ is independent of ν.

In combination, Eqs. (A4) and (A5) imply

$$\underset{z>0}{\text{Max}}\,|J_\nu(\nu z)| < C\,\nu^{-1/3} + \mathcal{O}(\nu^{-1/2}). \tag{A6}$$

References

1. J. R. Cary, J. D. Meiss, and A. Bhattacharjee, Phys. Rev. A 23, 2744 (1981).
2. J. R. Cary and J. D. Meiss, Phys. Rev. A 24, 2664 (1981).
3. B. V. Chirikov, Phys. Rep. 52, 263 (1979).
4. C. F. F. Karney, A. B. Rechester, and R. B. White, Physica D, 1982.
5. F. W. J. Olver, in Handbook of Mathematical Functions, M. Abramowitz and I. A. Stegun, eds. (Dover, New York, 1965) p. 355.
6. A. B. Rechester and R. B. White, Phys. Rev. Lett. 44, 1586 (1980).
7. A. B. Rechester, M. N. Rosenbluth, and R. B. White, Phys. Rev. A 23, 2664 (1981).

Figure Captions

Fig. 1 Trajectory in (j,ℓ) space for the principal term

Fig. 2 Trajectory containing one defect, as needed for the odd-k correlations.

Fig. 3 a)Correction to fourth characteristic function $\chi_4-\chi_4^P$ as a function of ε. Values of ε for which islands exist are shown by hatched regions on the axis. b) Maximum k for validity of even χ_k^P from Eq. (9).

Fig. 4 Absolute value of the force-correlation decay for the connected ergodic region of the standard map at $\varepsilon = 10.5$. Even-k theory is shown as a solid straight line. Numerical values not shown were consistent with zero.

Fig. 5 Absolute value of the force-correlation decay for the connected ergodic region of the standard map at $\varepsilon = 11.5$. Even-k theory is shown as a solid straight line. Numerical values not shown were consistent with zero.

Fig. 6 Absolute value of the force-correlation decay for the connected ergodic region of the standard map at $\varepsilon = 12.8$. Even-k theory is shown as a solid straight line. Numerical values not shown were consistent with zero.

Fig. 7 Ratio of observed diffusion constant to quasilinear value as a function of the nonlinearity parameter ε. Solid line is from Eq. (10) of the present work. Dashed line is $1 - 2J_2(\varepsilon)$.

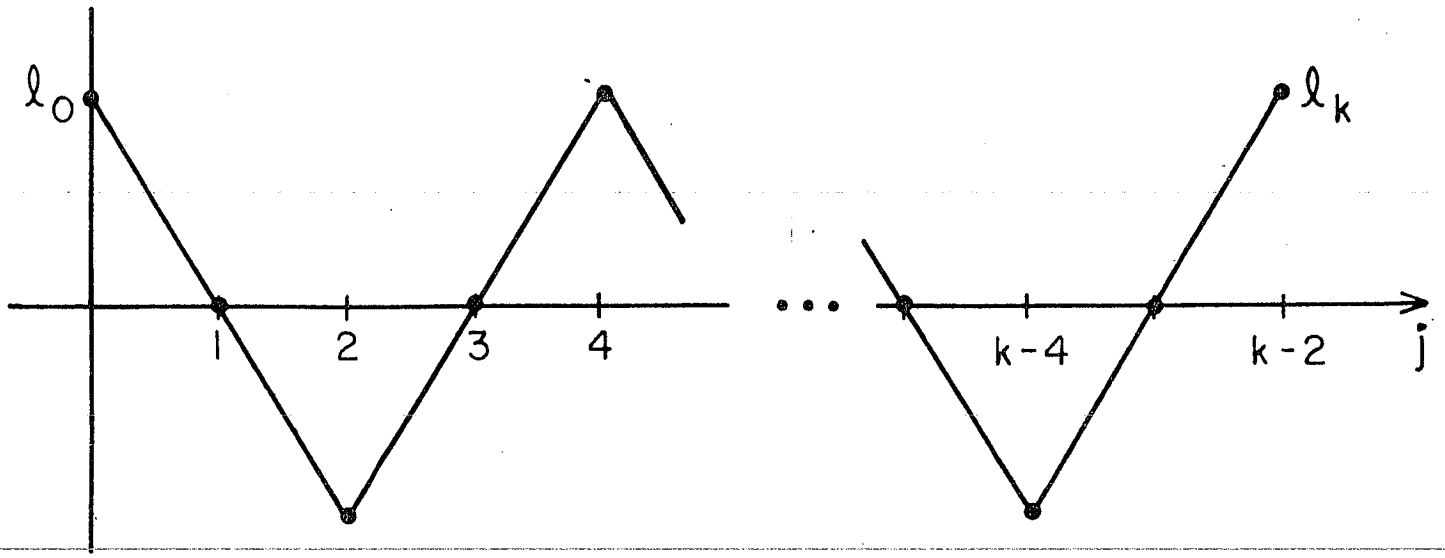

Fig. 1

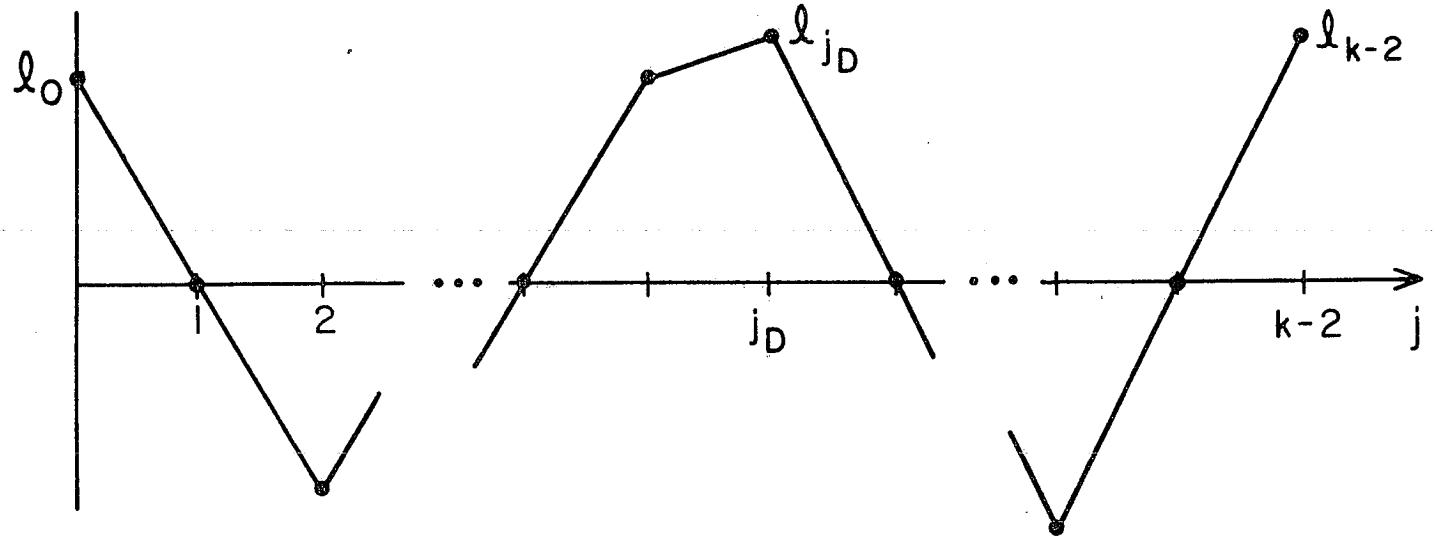

Fig.2

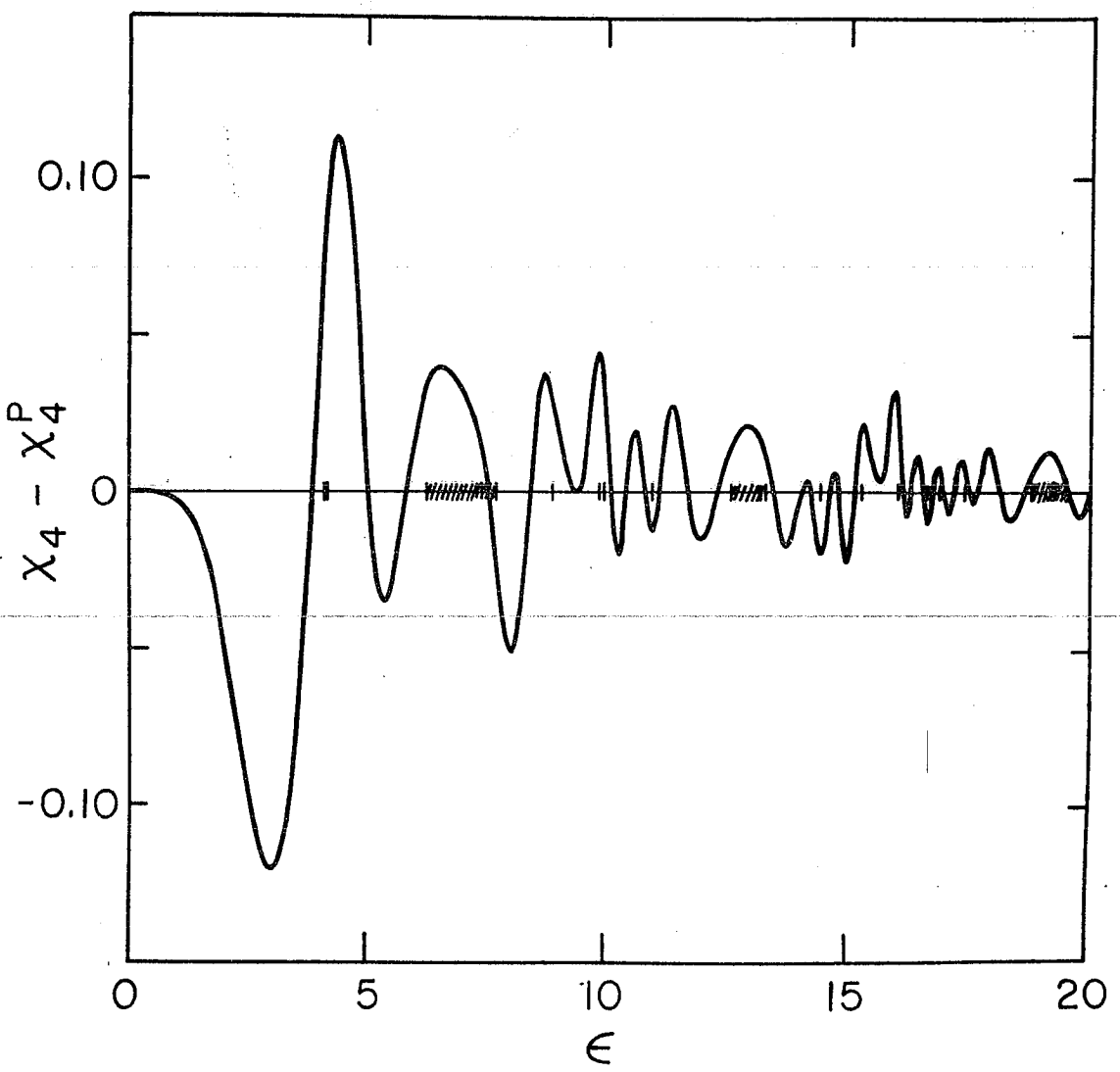

FIG. 3a

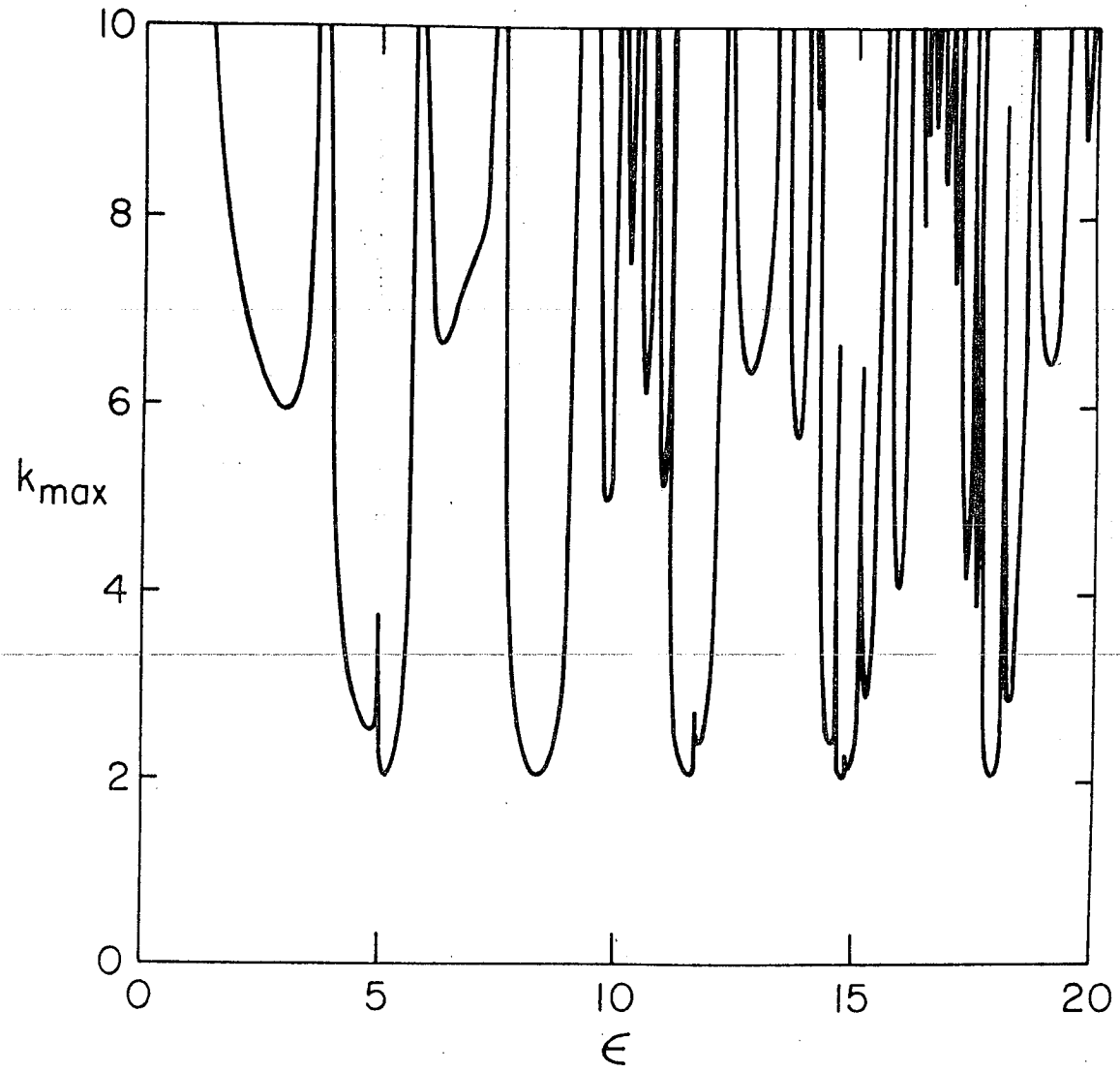

FIG. 3b

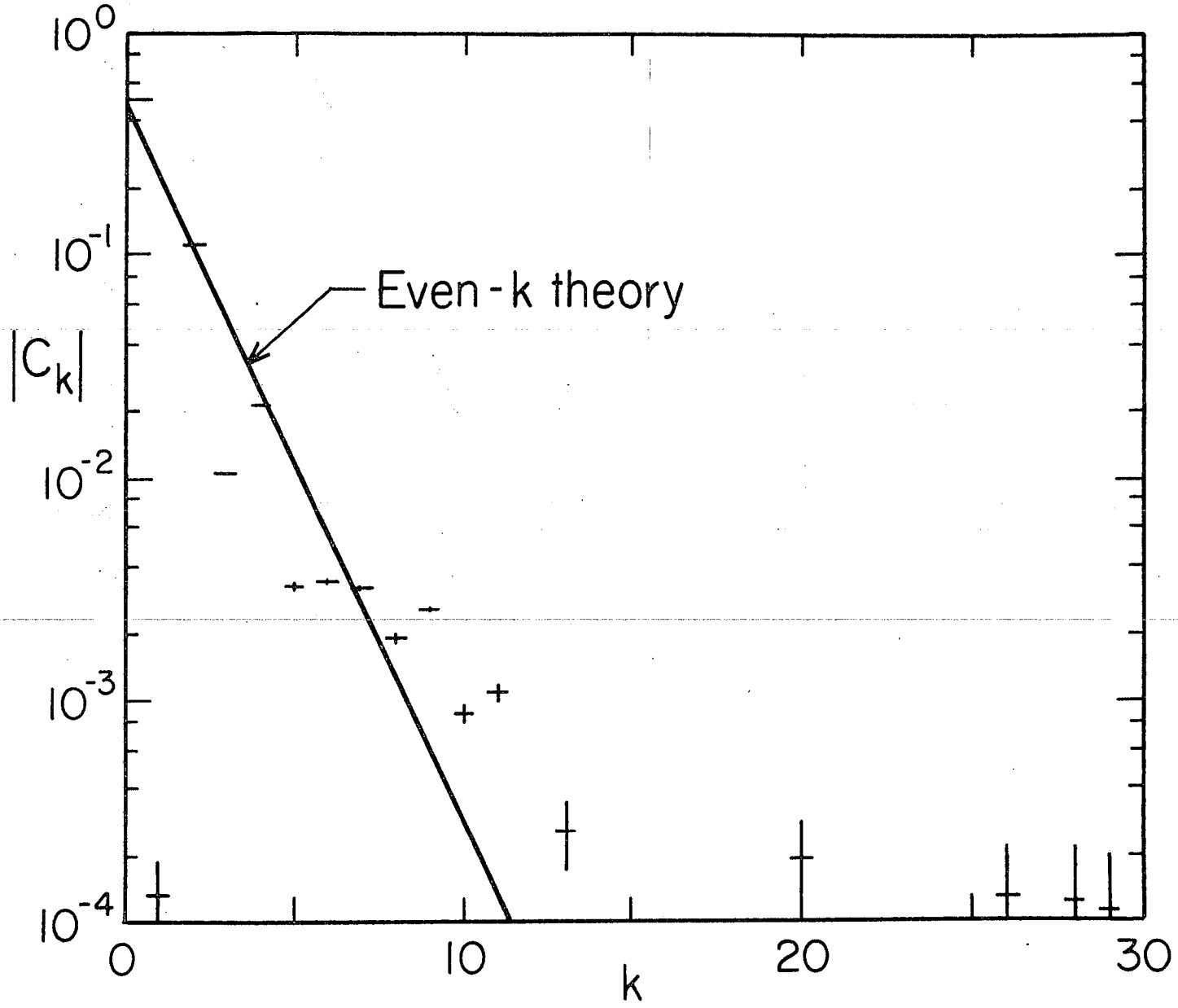

FIG. 4

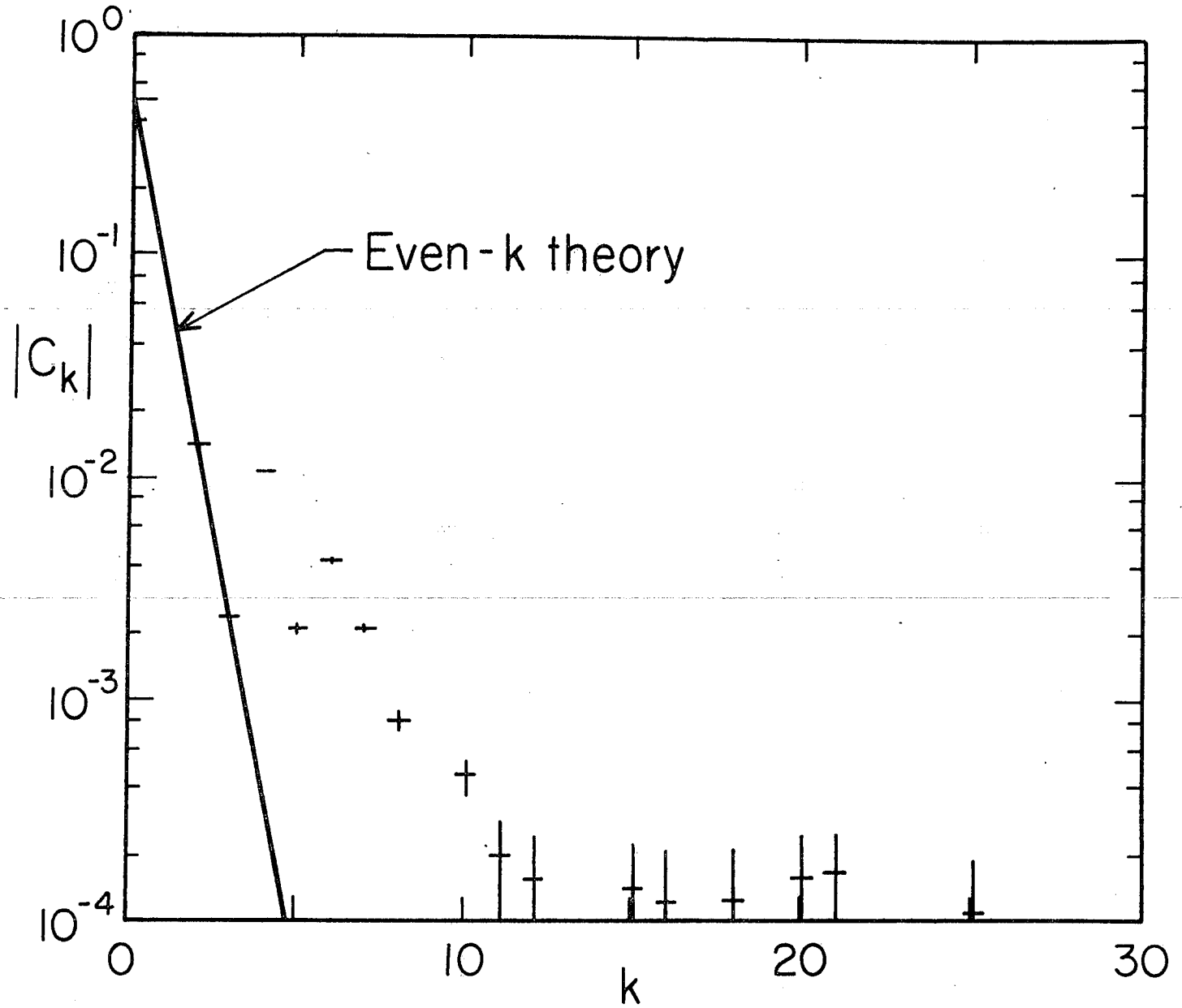

FIG. 5

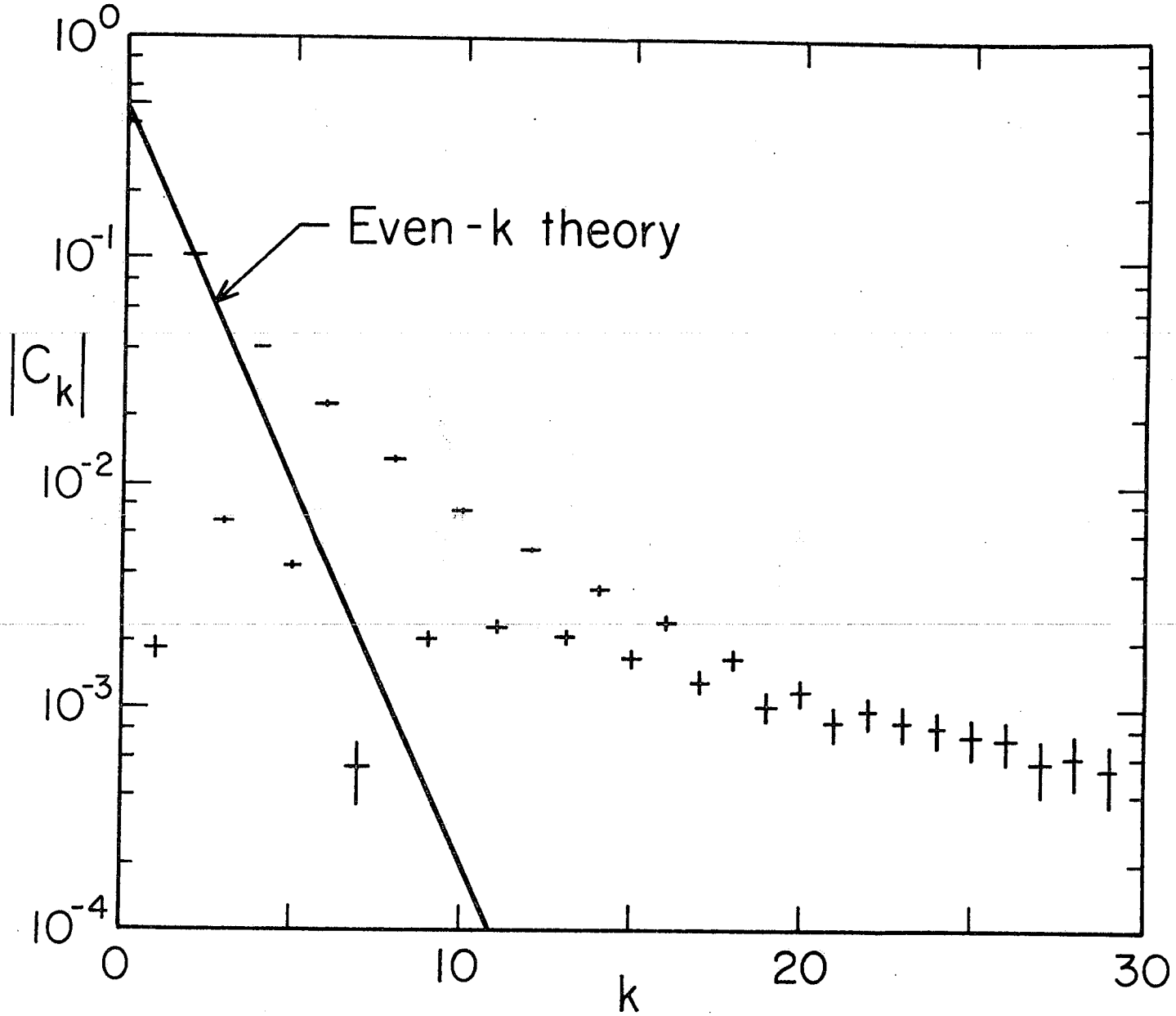

FIG. 6

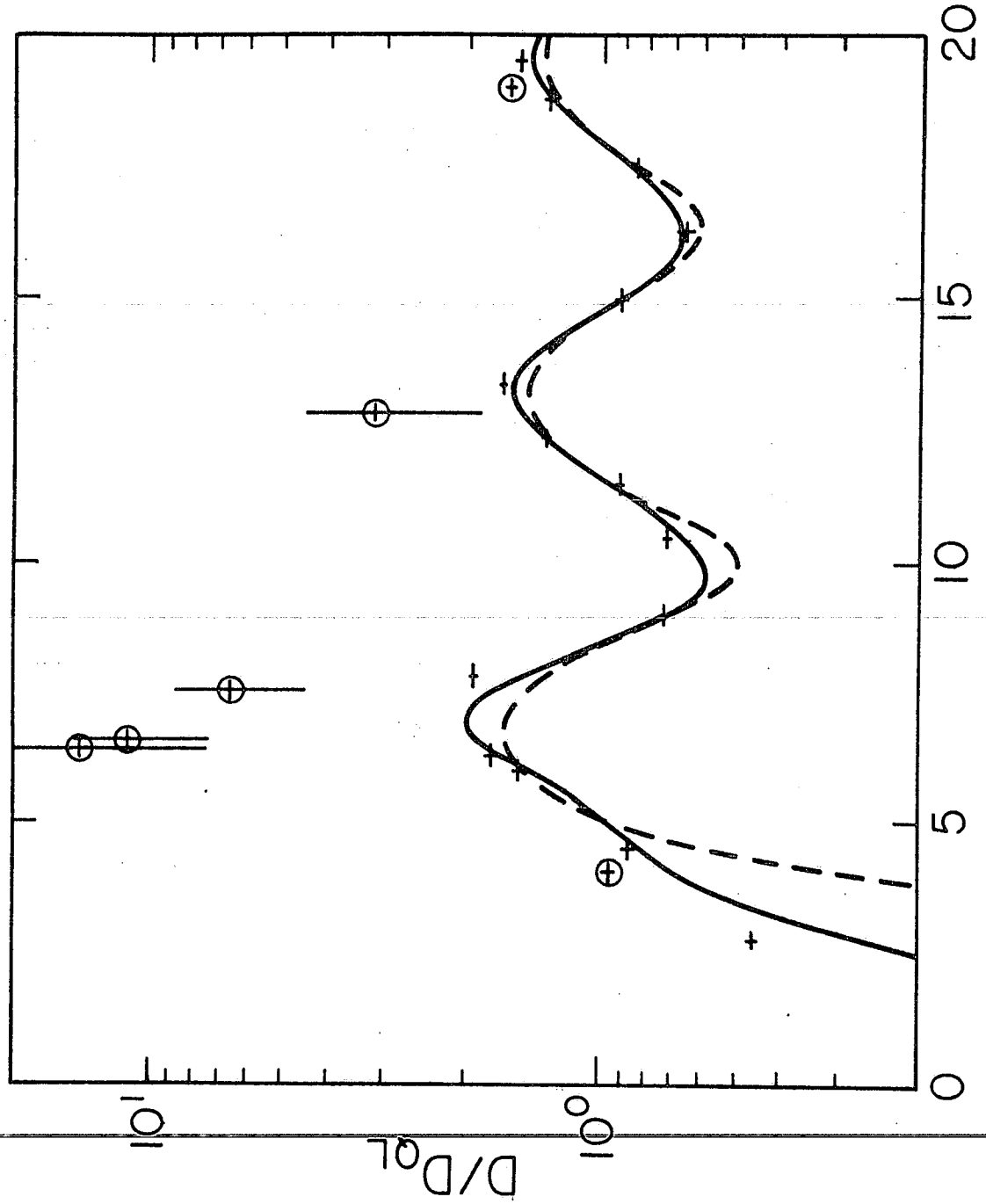

FIG. 7